Radiology Case Reports 16 (2021) 1965–1973

Available online at www.sciencedirect.com

ScienceDirect

journal homepage: www.elsevier.com/locate/radcr

Case Report

Relapsed Wilms' Tumor Presenting as Metastasis to the Zygoma ☆,☆☆,★

Ryan Thibodeau, MD, MPH[a,*], *Abtin Jafroodifar, MD*[a], *Marlon Coelho, MD*[a], *Hsin Kwung Li, MD*[b], *Lorenzo Gitto, MD*[c], *Daniel J. Zaccarini, MD*[c], *Mary McGrath, MD*[a]

[a] *Department of Radiology, SUNY Upstate Medical University, Syracuse, NY*
[b] *Department of Radiation Oncology, SUNY Upstate Medical University, Syracuse, NY*
[c] *Department of Pathology, SUNY Upstate Medical University, Syracuse, NY*

ARTICLE INFO

Article history:
Received 2 May 2021
Accepted 4 May 2021

ABSTRACT

Wilms' tumor accounts for the majority of renal tumors in children. Rarely, Wilms' tumor may metastasize to the bone. We present a case of a 15-month-old female who presented with severe abdominal distension and signs of cachexia. Abdominal ultrasonography and radiography of the abdomen both demonstrated a large abdominal mass. Follow-up computed tomography of the abdomen revealed a heterogeneous intra-abdominal mass arising from the left kidney which was surrounded by a thin rim of renal parenchyma. Biopsy of the mass revealed findings consistent with Wilms' tumor. The patient was 14 months status-post nephrectomy and chemoradiation but returned to the clinic with left facial swelling. Magnetic resonance imaging of the face demonstrated a multilobulated, heterogeneously enhancing solitary mass lesion in the left temple centered in the left zygoma with signs of bone breakdown. Despite its rarity, metastatic Wilms' tumor to bone should be considered in a child presenting with a new focal mass overlying bony-structures.

Introduction

Wilms' tumor (WT) accounts for up to 95% of renal tumors in children and is therefore the most common abdominal malignancy [1]. WT is an embryonal childhood tumor of metanephric origin and WT appears histologically similar to cells seen in the early stages of nephrogenesis [2]. Metastasis occurs in the minority of patients, most frequently to the lung parenchyma, and to a lesser extent the liver and regional

☆ Acknowledgements: none
☆☆ Competing Interest: The authors do not have any declarations to disclose.
★ Patient consent: No consent obtained for this case report as this is a retrospective study with no patient identifiers. "Formal consents are not required for the use of entirely anonymized images from which the individual cannot be identified - for example, x-rays, ultrasound images, pathology slides or laparoscopic images, provided that these do not contain any identifying marks and are not accompanied by text that might identify the individual concerned."

* *Corresponding author*.
E-mail address: thiboder@upstate.edu (R. Thibodeau).

https://doi.org/10.1016/j.radcr.2021.05.015

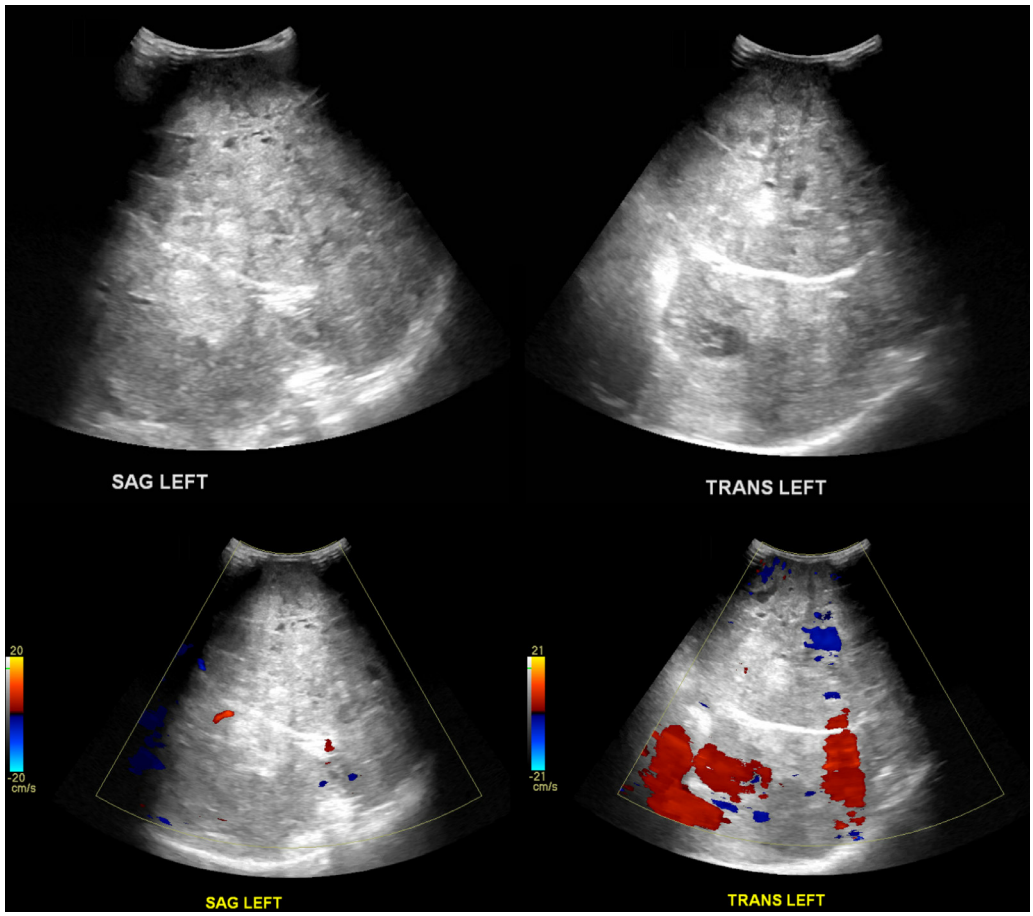

Fig. 1 – Ultrasound of the abdomen in both sagittal and transverse left views demonstrating a large heterogeneous mass in the central abdomen with internal blood flow.

lymph nodes. Rarely, WT may metastasize to unusual locations, such as the bone marrow, bones, and secretory glands [3]. Approximately 1.3% of patients with WT develop bone metastasis [4]. We present an unusual case of metastatic WT to the patients zygoma with local extension into the facial soft tissue.

Case presentation

The parents of a 15-month-old female brought the patient into the emergency department due to abdominal distension. Despite 2 months of attempting to change the patient's diet, they were concerned that the distension did not resolve, and that the patient appeared to have lost weight in her upper body. In the emergency department, the patient was febrile but responded appropriately to acetaminophen. The parents deny rash, nausea, vomiting, diarrhea, constipation, appetite changes, shortness of breath, lymphadenopathy, and edema. On physical exam, the patient was a nonverbal female with sunken eyes, no muscle tone in the upper extremities bilaterally, cachectic-appearing ribs visible over the chest, and had a large protruding abdomen. Laboratory evaluation showed hyponatremia, hyperkalemia, and very low hemoglobin (5.3 g/dL) and hematocrit (18.4%) but no leukocytosis. Radiologic imaging was ordered to evaluate the abdominal distension.

Abdominal ultrasound (Fig. 1) demonstrated a large, heterogeneous mass-like lesion in the central abdomen with internal blood flow. This lesion was too large to adequately evaluate with ultrasound. Abdominal radiography (Fig. 2) demonstrated bulging of the flanks bilaterally. Most of the bowel loops were displaced in the right abdomen due to the mass effect, but no evidence to suggest bowel obstruction. A follow-up computed tomography (CT) of the abdomen with contrast (Fig. 3) demonstrated a large, heterogenous intra-abdominal mass occupying most of the abdomen, measuring 18.3 × 13.6 × 14.2 cm. The mass arose from the left kidney and a thin rim of left renal parenchyma was identified on the posterior medial aspect of the mass. Moderate right hydronephrosis was present, which may be secondary to obstruction of the right ureter by the large intra-abdominal mass. The abdominal aorta and right kidney were displaced by the mass.

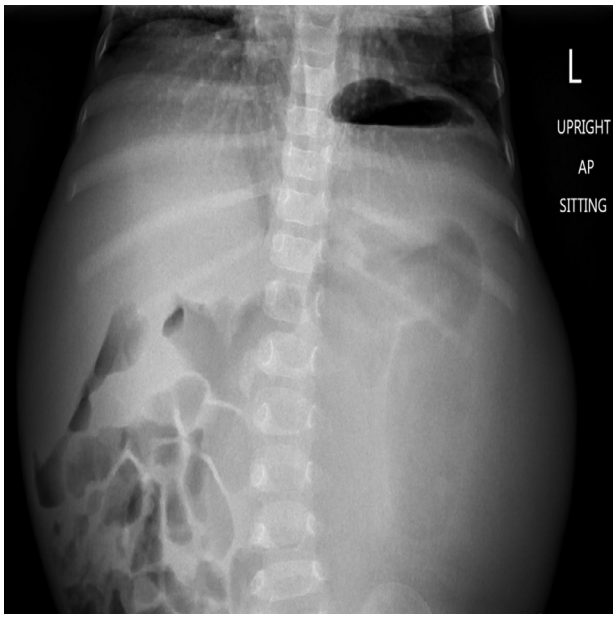

Fig. 2 – Upright sitting anterior-posterior radiography of the abdomen demonstrating bulging of the flanks bilaterally with displacement of the bowel loops to the right abdomen.

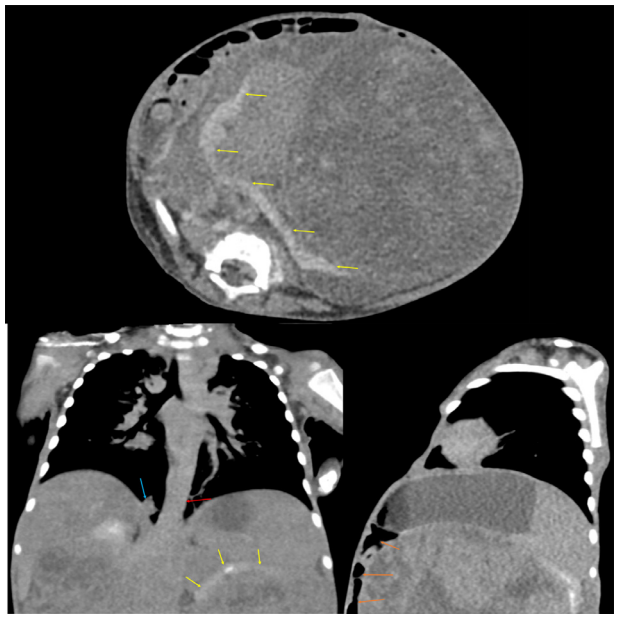

Fig. 3 – CT of the abdomen demonstrating a large, heterogeneous intra-abdominal mass occupying the majority of the abdomen. The mass is seen arising from the left kidney and a thin rim of left renal parenchyma (yellow arrows). Displacement of the abdominal aorta (red arrow) and bowels (orange arrows) is seen. A small nodular density in the medial aspect of the right lung base is seen (blue arrow). (Color version of figure is available online).

A small nodular density in the medial aspect of the right lung base was present. Further characterization of this nodule with CT of the thorax with intravenous contrast revealed the nodule measured 1.1 × 0.9 × 0.8 cm in the right lower lobe.

The patient was scheduled for a peripheral intra-arterial central catheter placement and image-guided left renal mass biopsy. Surgical pathology (Fig. 4) revealed a triphasic malignant neoplasm composed of blastema, epithelial elements, and myxoid stroma with immature spindle cells. Neoplastic cells exhibited moderate nuclear pleomorphism, individual cell necrosis, and numerous mitoses. Multipolar mitoses or nuclear features of anaplasia were not identified. Immunohistochemistry revealed positive expression of CD56 and WT-1 by the neoplastic cells, consistent with nephroblastoma (WT). Given the very large size of the tumor, she was not a surgical candidate. The patient was seen by the pediatric hematology-oncology service who treated the patient with 4 cycles of vincristine, 1 cycle of vincristine and dactinomycin, and 1 cycle of vincristine and doxorubicin.

The patient began to significantly improve following correction of her pre-admission malnutrition and tumor shrinkage secondary to chemotherapy. She was then seen by pediatric surgery and was found to now be a surgical candidate for excision/debulking procedure. She underwent an exploratory laparotomy and left nephrectomy, partial ureterectomy, and excision of retroperitoneal midline mass (presumed to be a paraaortic lymph node). The patient did well post-operatively. Surgical pathology of the intra-abdominal mass (Fig. 5) revealed findings consistent with WT, in addition to metastatic WT to the paraaortic lymph node. Cytogenomic microarray analysis using an Affymetrix OncoScan TM CNV array (Thermo Fisher Scientific, Waltham, MA, US) to detect copy number gains and losses, as well as regions of homozygosity (usually indicating loss of heterozygosity in tumor samples). In the DNA isolated from this patient's WT sample (estimated to be 70% tumor by pathology review), copy number loss/loss of heterozygosity for 1p and copy number gain of 1q was observed. Copy number loss/loss of heterozygosity for 16q was not observed. The patient then received radiotherapy to the whole abdomen to a dose of 1050 cGy in 150 cGy daily fractions (7 fractions total).

The patient did well for 14 months but returned to the pediatric hematology-oncology clinic presenting with a new facial swelling below the left eye. The mom reports that she noticed the swelling a couple of weeks prior and appears to be worse in the morning and gradually improved throughout the day. Parents deny any recent fever, eye pain, loss of appetite, and weight loss. The patient was able to move her eye without problems on physical exam.

Magnetic resonance imaging (MRI) of the face with and without intravenous contrast (Fig. 6) demonstrated a multilobulated, heterogeneously enhancing solitary mass lesion in the left temple centered in the left zygoma measuring approximately 3.1 cm x 2.5 cm x 3.0 cm. The mass was hypointense on T1-weighted imaging, hyperintense on T2-weighted imaging, and demonstrated significant diffusion restriction. The mass

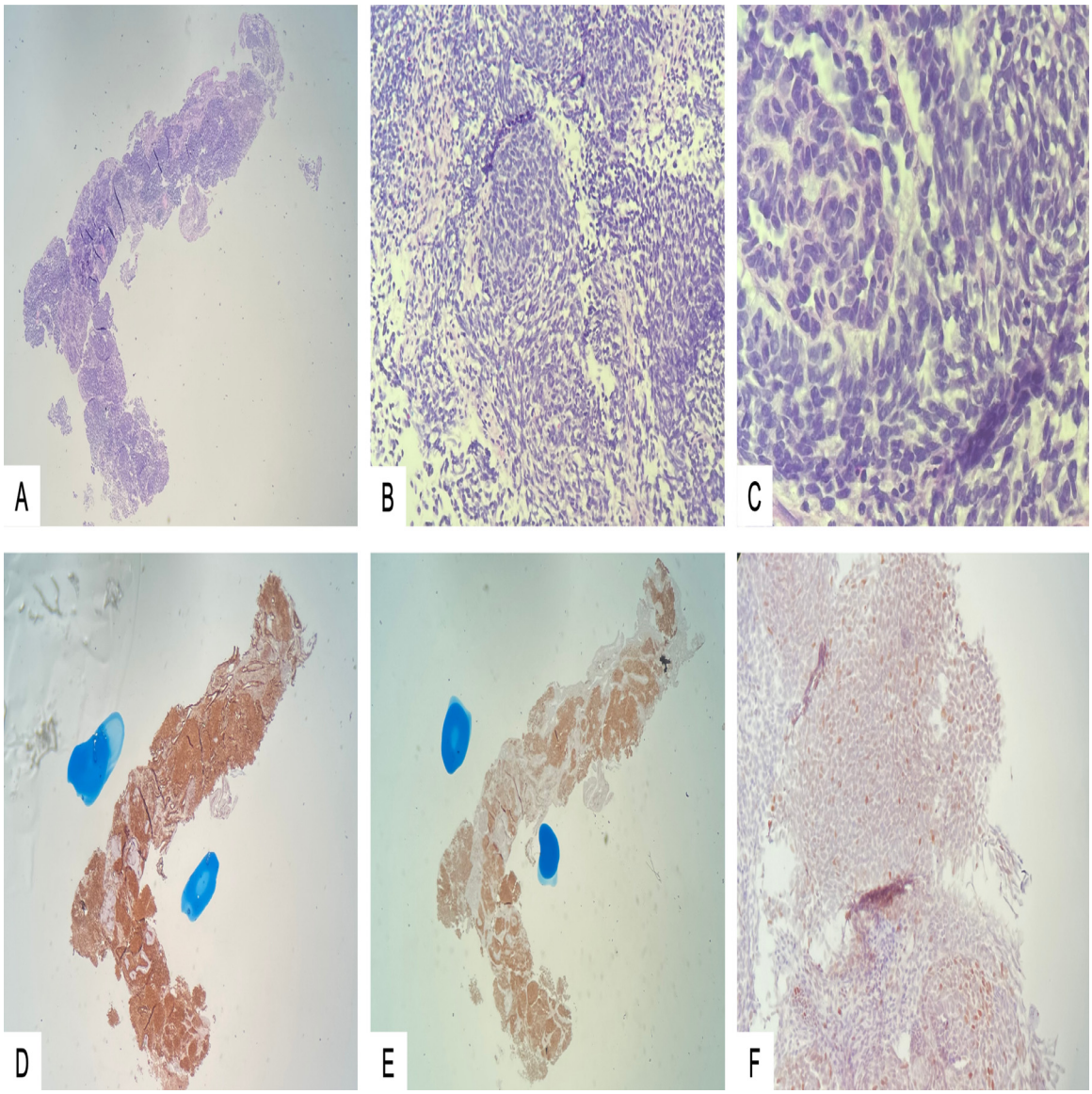

Fig. 4 – Microscopic examination showed a triphasic malignant neoplasm composed of blastema, epithelial elements, and myxoid stroma with immature spindle cells (H&E – A: 40X, B: 100X, C: 400X). Neoplastic cells exhibited moderate nuclear pleomorphism, individual cell necrosis and numerous mitoses. These cells stained diffusely positive for WT1 (D) and CD56 (E), and focally for P53 (F).

extended into the left peri-zygomatic soft tissues. There was mass effect with effacement of the left aspect of the extraconal fat abutting the globe and very mild left proptosis was noted. The extraocular muscles were symmetric and demonstrated normal morphology. No abnormalities were seen in the bilateral optic nerve sheath complexes or optic chiasm. There was no abnormal signal or abnormal enhancement of the brain parenchyma.

A biopsy of the facial mass was ordered. Pathology (Fig. 7) shows sections of bone involved by a small blue cell tumor with tubule formation and a stromal component. There is no evidence of anaplasia. The observed tumor cells appeared similar to the prior kidney tumor pathology. The tumor cells were negative for S100, p63, and WT-1. PAX-8 immunostain was positive in tumor cells, which supported the diagnosis of metastatic WT. Whole-body nuclear medicine bone scan with technetium-99m labeled with methylene diphosphonate and a CT of the thorax, abdomen, and pelvis did not show other areas of metastatic disease. The patient was scheduled for chemotherapy followed by radiation therapy. The simulation CT for radiation planning (Fig. 8) demonstrated an expansile osteolytic lesion measuring 3.0 × 2.2 cm within the left lateral orbit wall expanding into the temporal process of the zygomatic bone with notable

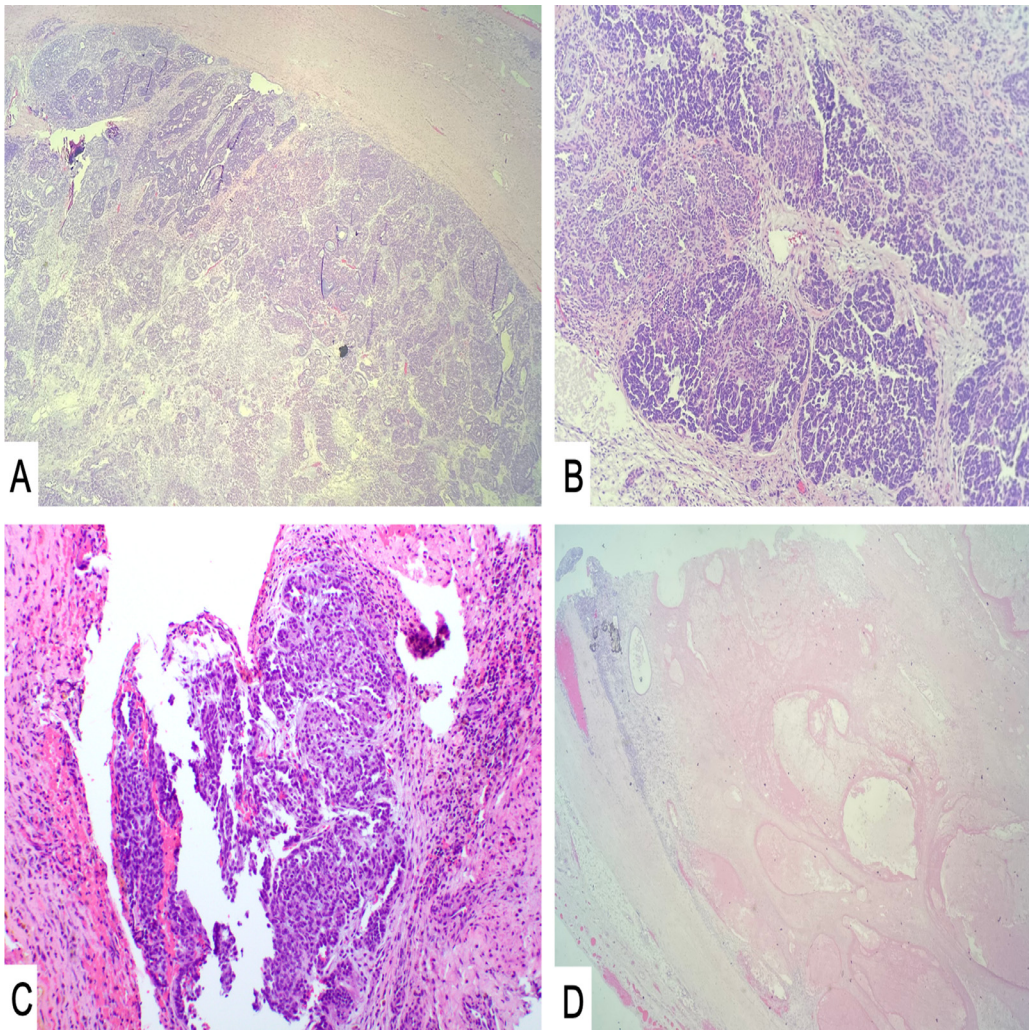

Fig. 5 – Sections of the main tumor excised after neoadjuvant chemotherapy. Microscopic examination revealed Wilms' tumor (H&E – A: 40X, B: 100X) composed of blastemal and epithelial cell types (C: H&E – 100X) in the background of extensive necrosis with treatment effect (D: 40X).

mass effect and distortion of the left lateral aspect of the left eye.

Discussion

The majority of patients with WT present with a solitary tumor. Patients may present with bilateral synchronous solitary tumors (57%) or multifocal tumors within a single kidney (10%) [5]. The vast majority of patients with WT present with an asymptomatic abdominal mass, though some patients (20%-30%) may present with signs and symptoms of abdominal pain, malaise, or microscopic or macroscopic hematuria [6]. Radiologic imaging plays an important role in diagnosing, locoregional staging, evaluation of distant metastatic disease, and surveillance of WT.

Initial imaging of a suspected renal mass consists of ultrasonography. If a renal mass is found, then the origin of the mass should be evaluated, though this may be difficult if the mass is retroperitoneal or there is anatomical distortion secondary to the mass. Renal masses tend to distort normal renal parenchyma and may move during normal respiratory cycles. On the contrary, renal masses that breach the renal capsule and invade adjacent structures may not move. On ultrasonography, WT may be variably echogenic depending on the degree of tissue necrosis and intratumoral hemorrhage. Evaluation of the contralateral kidney is important to assess for synchronous lesions [7]. It is essential to assess for local tumor spillage by imaging the liver and rectouterine pouch. In the setting where CT or MRI has not been utilized, intravascular extension into the renal vein and inferior vena cava may be evaluated using grayscale and color Doppler ultrasonography. Both ultrasonographic settings are needed as tumor thrombus

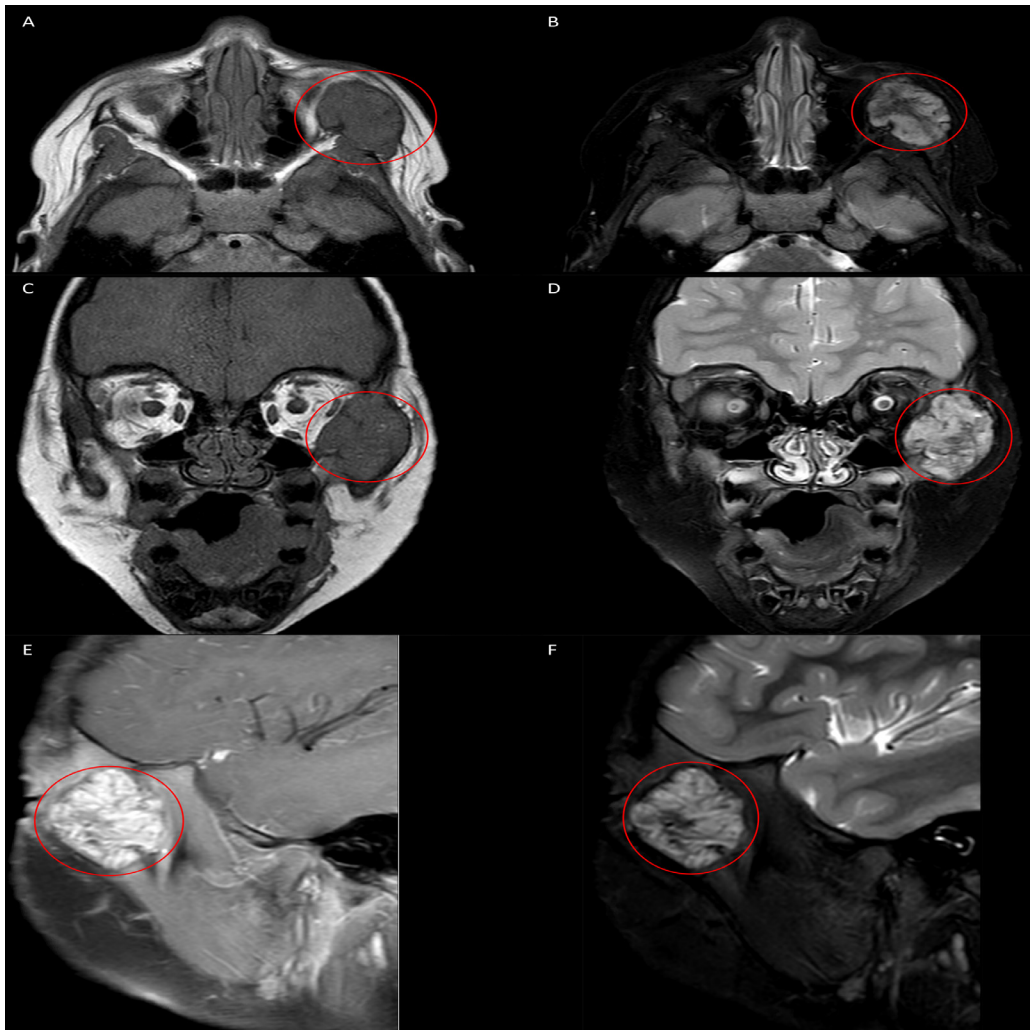

Fig. 6 – Axial (A, B), coronal (C, D), and sagittal (E, F) planes of a MRI of the face demonstrating a multilobulated, heterogeneously enhancing solitary mass centered within the left zygoma (red circles; A-F). The mass is seen extending into the left peri-zygomatic soft tissues with visible mass effect with effacement of the left aspect of the extraconal fat abutting the globe. T1-weighted imaging (A, C) demonstrates a hypointense lesion, while T2-weighted imaging (B, D) demonstrates a hyperintense lesion. Post-contrast images (E) reveal contrast uptake. Short tau intensity resonance imaging reveals a hyperintense lesion without peritumoral inflammation. (Color version of figure is available online).

secondary to intravascular extension may result in a falsely negative color Doppler evaluation [7,8].

Following ultrasonography, CT or MRI with contrast should be used for staging and pre-surgical planning. Since CT and MRI have been shown to be equivalent in diagnostic performance for locoregional staging, institutions may opt for either imaging modality. Evaluation using contrast-enhanced CT of the thorax is recommended given that the majority of metastatic WT is to the lung parenchyma and the addition of the contrast allows for proper evaluation of hilar and intravascular thrombus [3,7,9]. If MRI of the abdomen will be used for locoregional staging, then CT of the thorax should be preferentially completed before the MRI, especially if sedation is used [7,10]. If the decision for CT of the abdomen and pelvis is made, evaluation includes intravenous contrast in the portal venous phase. Oral contrast and multiphase CT scanning should be avoided due to its lack of added diagnostic benefit in children [7,11].

Metastasis of WT to the bone is rare. Marsden et al. used data from the Oxford survey of Childhood Cancer (1,368 patients) and found that the prevalence of bone metastasis was 1.3%, where the most common site was the spine [4]. Bond and Martin performed a similar study with 1,267 patients and found that 3.5% of patients developed bone metastasis without a predilection for the involved site [12]. Data from both patient datasets revealed that patients with bone metastasis had a poor prognosis. Bond and Martin reported 1 survivor (2.2%) while Marsden et al. did not report any survivors [4,12]. This is

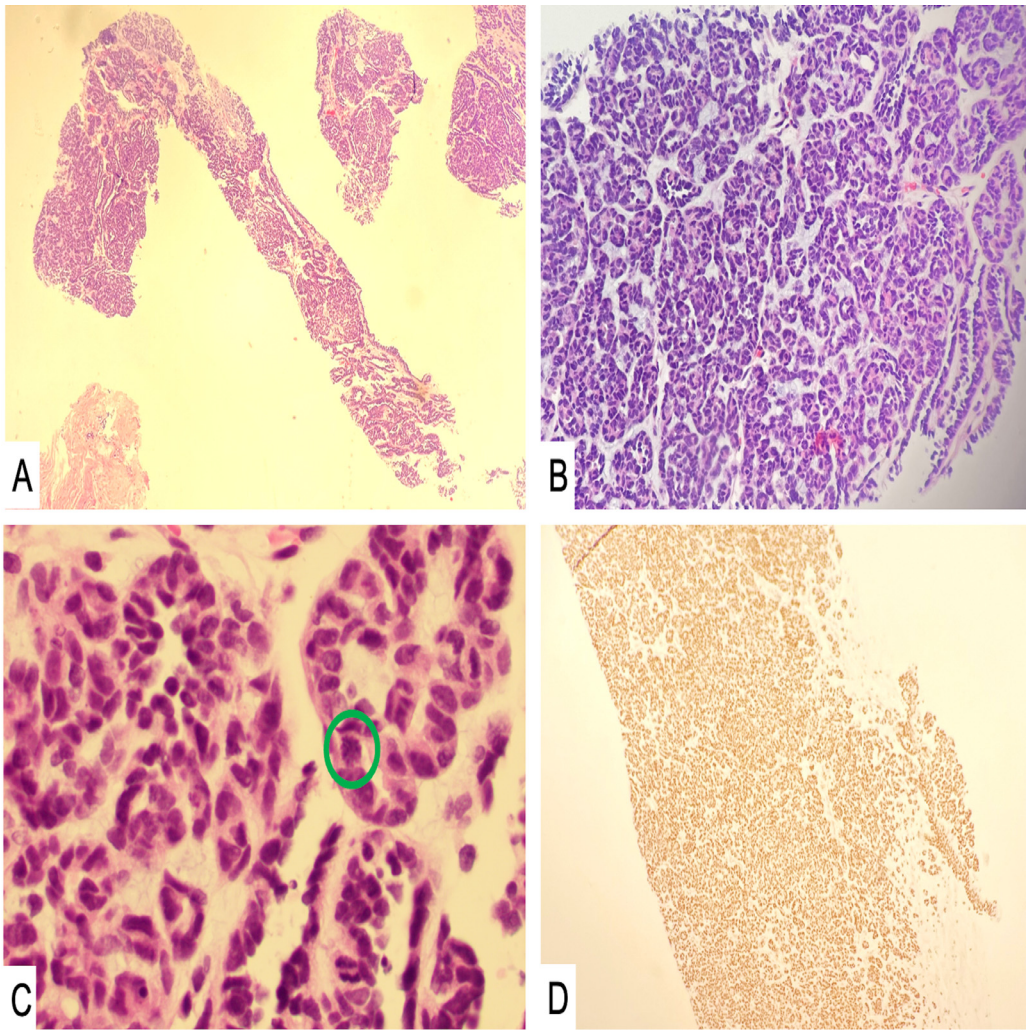

Fig. 7 – Microscopic examination showed bone involvement with a small blue cell tumor with tubule formation and a stromal component (A, B – H&E, 40X and 100X). Occasional mitoses were observed (C, green circle – H&E, 400X). The tumor cells stained positive for PAX-8 (D) and negative for S100, p63, and WT-1, supporting the diagnosis of metastatic Wilms tumor.

in stark contrast to non-metastatic WT and metastatic WT to the lung which both have excellent 5-year survival and overall survival rates [13].

Metastatic WT bone lesions appear as osteolytic bone lesions on radiography. On CT, these lesions also appear lytic, either represented as a permeative process ("moth-eaten appearance") or geographic bone destruction. These lesions appear radiologically aggressive and tend to have poorly-defined margins [12]. In our patient, the WT bone lesions were represented as a heterogeneously enhancing solitary mass that is hyperintense on T2-weighted imaging surrounded by boney destruction on MRI.

Fortunately, the overall survival of children with WT is over 90%, although certain molecular characteristics have been associated with worse prognosis (such as copy number gain of 1q and diffuse P53 staining) [13-15]. Approximately 15% of children treated for WT will relapse (usually <2 years after diagnosis), most commonly in the lungs (58%) and abdomen (29%) [16-18]. Given these data, patients should be followed closely with surveillance imaging to detect asymptomatic tumor relapse or metastasis. The Children's Oncology Group recommends abdominal evaluation with CT or MRI of the abdomen for the first 2 years following treatment, along with CT of the thorax for the first 2-3 years and then switching to chest radiography. Though, recent data from Mullen et al. revealed no difference in overall survival when comparing CT from chest radiography and ultrasonography despite a shorter median time detection from diagnosis to recurrence by CT [19]. Despite some studies showing there may be benefit for nuclear medicine surveillance imaging, there are no official recommendations [20,21].

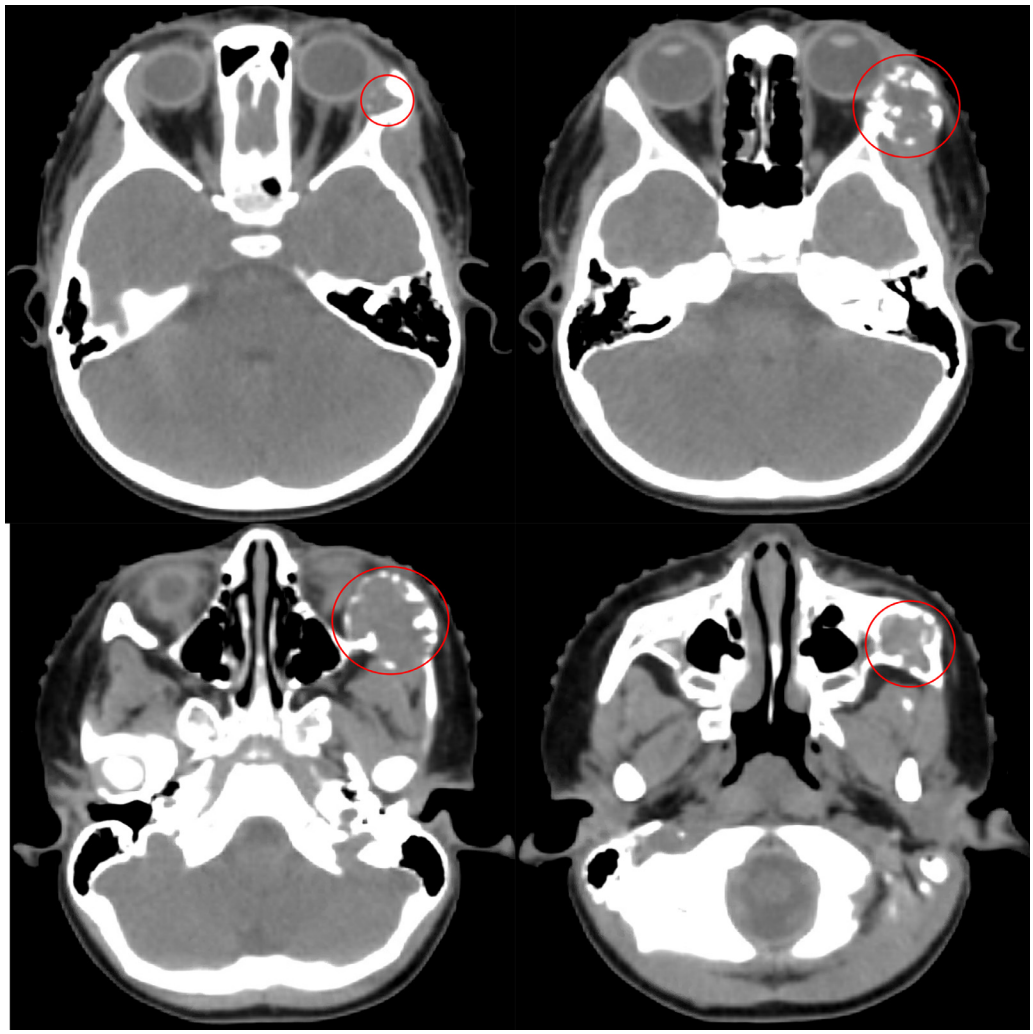

Fig. 8 – Radiation oncology simulation CT of the head demonstrating an expansile osteolytic lesion (red circle) within the left lateral orbital wall extending to the temporal process of the zygomatic bone. (Color version of figure is available online).

Conclusion

Wilms' tumor has an excellent overall survival. However, metastatic Wilms' tumor, especially to bone, bears a significantly worse prognosis. Bone lesions are usually demonstrated as osteolytic lesions on radiography and computed tomography and hyperintense mass on T2-weighted magnetic resonance imaging. Surveillance imaging using cross-sectional imaging or radiography has been shown to improve overall survival.

REFERENCES

[1] Phelps HM, Kaviany S, Borinstein SC, Lovvorn HN. Biological drivers of Wilms' tumor prognosis and treatment. Child 2018;5(11). doi:10.3390/children5110145.

[2] Treger TD, Chowdhury T, Pritchard-Jones K, Behjati S. The genetic changes of Wilms' tumour. Nat Rev Nephrol 2019;15(4):240–51. doi:10.1038/s41581-019-0112-0.

[3] Al-Hadidi A, Lapkus M, Novotny NM, Gowans LK, Chen PY, Stakkuib A. Wilms' tumor with pleural metastasis. Glob Pediatr Heal 2020;7(2333794X20952292). doi:10.1177/2333794X20952292.

[4] Marsden HB, Lennox EL, Lawler W, Kinnier-Wilson LM. Bone metastases in childhood renal tumours. Br J Cancer 1980;41(6):875–9. doi:10.1038/bjc.1980.163.

[5] Charlton J, Irtan S, Bergeron C, Pritchard-Jones K. Bilateral Wilms' tumour: a review of clinical and molecular features. Expert Rev Mol Med 2017;19:e8. doi:10.1017/erm.2017.8.

[6] Davidoff AM. Wilms' tumor. Adv Pediatr 2012;59(1):247–67. doi:10.1016/j.yapd.2012.04.001.

[7] Servaes SE, Hoffer FA, Smith EA, Khanna G. Imaging of Wilms' tumor: an update. Pediatr Radiol 2019;49(11):1441–52. doi:10.1007/s00247-019-04423-3.

[8] Ritchey ML, Othersen HBJ, de Lorimier AA, Kramer SA, Benson C, Kelalis PP. Renal vein involvement with nephroblastoma: a report of the National Wilms' Tumor Study-3. Eur Urol 1990;17(2):139–44. doi:10.1159/000464022.

[9] Khanna G, Rosen N, Anderson JR, Ehrlich PF, Dome JS, Gow KW, et al. Evaluation of diagnostic performance of CT for detection of tumor thrombus in children with Wilms'

tumor: a report from the children's oncology group. Pediatr Blood Cancer 2012;58(4):551–5. doi:10.1002/pbc.23222.
[10] Servaes S, Khanna G, Naranjo A, Geller JI, Ehrlich PF, Gow KW, et al. Comparison of diagnostic performance of CT and MRI for abdominal staging of pediatric renal tumors: a report from the children's oncology group. Pediatr Radiol 2015;45(2):166–72. doi:10.1007/s00247-014-3138-2.
[11] Just da Costa e Silva E, Alves Pontes da Silva G. Eliminating unenhanced CT when evaluating abdominal neoplasms in children. Am J Roentgenol 2007;189(5):1211–14. doi:10.2214/AJR.07.2154.
[12] Bond J V, Martin EC . Bone metastases in Wilms' tumour. Clin Radiol 1975;26(1):103–6. doi:10.1016/s0009-9260(75)80023-7.
[13] Dome JS, Fernandez C V, Mullen EA, Kalapurakal JA, Geller JI, Huff V, et al. Children's oncology group's 2013 blueprint for research: renal tumors. Pediatr Blood Cancer 2013;60(6):994–1000. doi:10.1002/pbc.24419.
[14] Gratias EJ, Dome JS, Jennings LJ, Chi YY, Tian J, Anderson J, et al. Association of chromosome 1q gain with inferior survival in favorable-histology Wilms tumor: a report from the children's oncology group. J Clin Oncol 2016;34(26):3189–94 Epub 2016 Jul 11. PMID: 27400937; PMCID: PMC5012705. doi:10.1200/JCO.2015.66.1140.
[15] Ooms AH, Gadd S, Gerhard DS, Smith M, Guidry Auvil J, Meerzaman D, et al. Significance of TP53 mutation in wilms tumors with diffuse anaplasia: a report from the children's oncology group. Clin Cancer Res 2016;22(22):5582–91. doi:10.1158/1078-0432.CCR-16-0985.
[16] Grundy P, Breslow N, Green DM, Sharples K, Evans A, D'Angio GJ. Prognostic factors for children with recurrent Wilms' tumor: results from the Second and Third National Wilms' Tumor Study. J Clin Oncol Off J Am Soc Clin Oncol 1989;7(5):638–47. doi:10.1200/JCO.1989.7.5.638.
[17] Grundy P, Perlman E, Rosen NS, Warwick AB, Glade Bender J, Ehrlich P, et al. Current issues in Wilms' tumor management. Curr Probl Cancer 2005;29(5):221–60. doi:10.1016/j.currproblcancer.2005.08.002.
[18] Brok J, Lopez-Yurda M, Tinteren H V, Treger TD, Furtwängler R, Graf N, et al. Relapse of Wilms' tumour and detection methods: a retrospective analysis of the 2001 renal tumour study group-international society of paediatric oncology Wilms' tumour protocol database. Lancet Oncol 2018;19(8):1072–81. doi:10.1016/S1470-2045(18)30293-6.
[19] Mullen EA, Chi Y-Y, Hibbitts E, Anderson JR, Steacy KJ, Geller JI, et al. Impact of surveillance imaging modality on survival after recurrence in patients with favorable-histology Wilms' tumor: a report from the children's oncology group. J Clin Oncol Off J Am Soc Clin Oncol 2018;36(34):JCO1800076. doi:10.1200/JCO.18.00076.
[20] Moinul Hossain AKM, Shulkin BL, Gelfand MJ, Bashir H, Daw NC, Sharp SE, et al. FDG positron emission tomography/computed tomography studies of Wilms' tumor. Eur J Nucl Med Mol Imaging 2010;37(7):1300–8. doi:10.1007/s00259-010-1396-2.
[21] Gururangan S, Wilimas JA, Fletcher BD. Bone metastases in Wilms' tumor–report of three cases and review of literature. Pediatr Radiol 1994;24(2):85–7. doi:10.1007/BF02020158.